Chris Koran
Aurélie Desrosiers

Directed Evolution of the Fluorescent Protein mNeonGreen

Final Lab Report

Report presented to
Professor Arnold Hayer
BIOL 301

McGill University
December 8, 2025

Abstract

Fluorescent proteins are widely used in modern biology, but even small sequence changes can noticeably affect brightness and stability. In this experiment, we tested whether random mutagenesis of mNeonGreen could generate variants with altered fluorescence properties. We created mutant libraries using EP-PCR, cloned the products into an expression plasmid, transformed *E. coli*, and screened colonies for differences in fluorescence. Candidate variants were then validated by restriction analysis and Sanger sequencing, and structural effects were explored with protein modeling. To connect colony-level screening to protein-level behavior, we also compared expression by Western blot and measured fluorescence properties using purified protein.

Two mutants were selected for further detailed characterization. M3 contained three amino-acid substitutions (L19M, A192V, M231V) and showed fluorescence behavior that was statistically similar to the wild-type across all of the metrics tested. In contrast, M4 carried a single substitution (I67T) near the chromophore pocket and showed clear detrimental changes. The fluorescence intensity was significantly reduced, excitation and emission maxima were significantly shifted, pKa increased, and photobleaching behavior differed from the wild-type. Western blot results indicated that M4 expressed at lower levels than wild-type or M3, suggesting that reduced expression likely contributed to the weaker signal in addition to changes in photophysical properties.

Taken together, our results show that random mutagenesis can produce mNeonGreen variants with statistically significant functional differences, but beneficial improvements were not recovered in this first round. The strong effect of the I67T substitution also suggests that chromophore-proximal residues are sensitive targets during fluorescent protein mutagenesis.

(249 words)

Introduction and aims

Fluorescent proteins enable the visualization of proteins in living cells and tracking of their dynamics over time. They drive quantitative applications such as protein tagging, biosensing, and live-cell imaging, allowing experiments to compare signals across different conditions while keeping cells viable.[1] Even among high-quality fluorescent proteins, properties like brightness, maturation rate, and resistance to photobleaching can vary enough to influence how clearly experiments can be interpreted from fluorescent imaging.[1] As a result, improving fluorescent protein performance through engineering and mutagenesis remains a major focus in cell-biology experiments.

Enhanced Green Fluorescent Protein (EGFP) has historically served as a benchmark for green fluorescent proteins due to its combination of high brightness, monomeric behavior, reliable folding (at 37°C), and broad compatibility with fusion tagging. Its use across imaging, biosensing, and high-throughput screening experiments means that many researchers

compare new fluorescent proteins directly to EGFP to determine whether a variant shows a significant improvement.[1,3] Thus, EGFP's performance provides a practical point of comparison when assessing next-generation fluorescent proteins such as mNeonGreen. Because EGFP has historically served as the standard for green fluorescent proteins, demonstrating that mNeonGreen exceeds EGFP in brightness and maturation directly highlights the significance of engineering improvements.

mNeonGreen (mNG), engineered from the lancelet protein LanYFP, is a good starting point for future fluorescence-based experiments. It produces a monomeric yellow-green fluorescent protein that substantially outperforms EGFP in brightness and maturation, while maintaining good photostability.[2] These properties have contributed to mNeonGreen's use for fusions, biosensors, Fluorescence Resonance Energy Transfer (FRET), and high-resolution imaging.[2] Even with its strong performance, past protein engineering work has shown that these targeted amino acid substitutions (particularly near the chromophore or in regions influencing folding) can significantly shift the brightness and photostability in fluorescent proteins.[1,3] This suggests that some unexplored regions of mNeonGreen's sequence space can still yield variants with altered and sometimes enhanced properties.

To explore this space, we used error-prone PCR (EP-PCR) to introduce random point mutations across the mNeonGreen coding sequence. EP-PCR increases the error rate of DNA polymerase (typically through the addition of $MnCl_2$ or $MgCl_2$), thereby generating diverse variant libraries suitable for directed evolutionary experiments aimed at improving protein function.[4] The resulting mNeonGreen variants were cloned into a pUC18-His plasmid vector and introduced into chemically competent *E. coli* for screening. Colony fluorescence on agar plates served as an initial indicator of altered brightness, allowing us to identify variants that had different fluorescence from the wild type mNeonGreen. The clones were then validated by restriction digest and Sanger sequencing to confirm correct plasmid insertion and map the mutations responsible for changes in brightness.

To keep screening meaningful, we treated colony fluorescence as apparent brightness, which quantifies the differences in expression level, folding efficiency, maturation, and photostability under our plate conditions. Chosen candidates differed the most significantly from wild-type mNeonGreen brightness.

Our goals were to (i) generate a diverse mNeonGreen mutant library, (ii) identify candidate variants with altered fluorescence intensity from plate images, (iii) confirm cloning and map mutations by restriction digest and Sanger sequencing, and (iv) choose a variant for later biophysical characterization based on the screening performance.

Our working hypothesis was that random substitutions would yield variants with measurable changes in brightness, and that some would outperform the wild-type in brightness during screening.[3]

(551 words)

Materials and methods

EP-PCR

Error prone PCR was performed on wildtype mNeonGreen template with increased concentrations of $MgCl_2$ [5.5 mM] and $MnCl_2$ [0.25 mM]. The EP-PCR product was digested with Dpnl enzyme to degrade the DNA template.

Purification

DNA was purified using a column-based purification kit, following manufacturer guidelines. For DNA sequencing, a silica gel-based spin column was used to purify plasmid DNA, following manufacturer guidelines.
Proteins were purified using affinity-purification. First, total cell lysates were prepared by suspending transformed E. coli in a lysis buffer (50 mM Tris-HCl pH 7.5, 200mM NaCl, 1mM DTT, 1mL/100mL (v:v) protease cocktail inhibitor, 5% (v:v) glycerol, 2% (v:v) Triton X-100, 2% (v:v) Tween20, 500 µg/ml lysozyme, 5 µl/ml $MgCl_2$, 10µl/ml RNase/DNase). Then, mNeonGreen proteins were purified using a His-tag-nickel-ion-based affinity purification method as per manufacturer guidelines. Protein concentrations were determined using the Bradford method.

Gel Electrophoresis

DNA samples were run in a 1% agarose gel containing Fluo-DNA in TAE buffer (40mM Tris-Acetate, 1mM EDTA). Band sizes were assessed with the GeneRuler 1kb DNA ladder. ChemiDoc was used to capture images of gels and plates.

Cloning

Products and pUC18-His vector were digested with XbaI and SacI restriction enzymes. Products were purified. pUC18-His was treated with phosphatase. Products and pUC18-His were ligated using T4 ligase. The resulting plasmid, encoding mutated mNeonGreen with an N-terminal 6xHis tag, was transformed into a chemically competent DH10β strain of *E. coli* using heat shock protocol at 42°C for 90 seconds. Transformed cells were selected on LB agar plates containing 100 µg/mL ampicillin at 37°C for 16 to 20 hours.
The pUC18-His-MutantmNeonGreen plasmid was digested with KpnI and XmnI restriction enzymes and agarose gel electrophoresis was subsequently performed to confirm cloning. Mutant candidates were selected by fluorescence intensity measured from images using FIJI. Samples were submitted to Genome Québec for Sanger sequencing using M13F primers.

Spectrofluorimetry

A spectrofluorometer was used to measure purified protein fluorescence. Analysed protein samples had a concentration of 7.5 μg/mL. Fluorescence intensity was measured at 495 nm (±10 nm) excitation and 520 nm (±10 nm) emission settings. The excitation spectrum was determined by measuring emission at 530 nm (±10 nm), while varying the excitation from 450-510 nm. The emission spectrum was determined by measuring emission from 500-550 nm, while excitation light was maintained at 480 nm (±10 nm). Fluorescence intensity was measured, using 495 nm (±10 nm) excitation and 520 nm (±10nm) emission settings, from proteins at pH values adjusted to 4.5, 5.5, 6.5, and 7.5 to determine pKa.

Western blot

Protein samples were heated at 95°C for 5 minutes. SDS-PAGE was performed using a 4-15% acrylamide gel. 20 μg of protein was loaded in the total lysate lanes and 1 μg of protein in the purified protein lanes. The separated proteins were transferred and immobilized on a PVDF membrane using the semi-dry transfer method. The membrane was probed with a mouse anti-His primary antibody. Then it was incubated in a blocking buffer (TBS-T + 7% (w/v) non-fat dry milk) and washed. The membrane was probed with a rabbit anti-mouse IgG secondary antibody conjugated with horseradish peroxidase (HRP). The membrane was subsequently incubated with HRP substrate (Clarity Western ECL substrate) and imaged using ChemiDoc.

Fluorescence microscopy

Transformed *E. coli* cells on top of an agarose gel pad were imaged using a fluorescence microscope. Pictures were taken every 2 seconds for a total of 60 images to determine the bleaching half-time.

Modelling

NBCI BLAST was used to align the wildtype and mutant mNeonGreen sequences and identify mutations. ExPASy translate was used to convert nucleotide sequences into protein sequences. Swiss Model was used to predict protein structure for protein sequences, using the 5LTR1.A. template for modelling. PyMol was used to visualize the protein structures predicted by Swiss Model, and to identify the location of the mutated amino acids.

(650 words)

Results

mNeonGreen was successfully amplified using error prone PCR.

To generate diverse mNeonGreen mutants, error prone PCR was performed on wild-type mNeonGreen template. The presence of mNeonGreen EP-PCR products was confirmed by the presence of a single band at approximately 720 bp in agarose gel electrophoresis in the EP-PCR product lanes, which corresponds the expected size of the mNeonGreen gene (Fig. 1). No bands were observed in the negative control lane.

mNeonGreen EP-PCR products were cloned and expressed in *E. coli.*

Transformed cells containing a vector-mNeonGreen product were selected on agar plates containing ampicillin. Colonies containing mNeonGreen were identified by fluorescence. The presence of many colonies growing on agar plates containing ampicillin confirmed the transformation of the vectors into *E. Coli* (Fig. 2A). Three non-fluorescent colonies were present on the vector only plate. The fluorescence of colonies confirmed the presence of mNeonGreen EP-PCR product in the transformed cells (Fig. 2B). The plate with wild-type mNeonGreen vectors had the highest proportion of strongly fluorescent colonies than the plates with EP-PCR product mNeonGreen vectors, which had variable fluorescence.

mNeonGreen EP-PCR products were ligated into pUC18-His plasmid vector.

To validate that mNeonGreen EP-PCR products were inserted, in the desired orientation, into the pUC18-His vector transformed into *E. coli*, silica gel-based spin column purification was performed followed by restriction enzyme digests with KpnI and XmnI. The ligation of mNeonGreen EP-PCR products into the pUC18-His vector was confirmed by the presence of a single band at 3400 bp in agarose gel electrophoresis in the lanes of wild-type and mutant mNeonGreen vectors digested with KpnI, corresponding to the expected size of the pUC18-His-mNeongreen vector (Fig. 3). The vector only, digested with KpnI, lane presented multiple faint nonspecific bands ranging from 2000 to 2600 bp. The orientation of mNeonGreen EP-PCR products in pUC18-His from the SacI to the XbaI restriction site was confirmed by the presence of two bands at 1400 and 2000 bp in agarose gel electrophoresis in the lanes of wild-type and mutant mNeonGreen vectors digested with KpnI and XmnI (Fig. 3). The lane of pUC18-His only vector digested with KpnI and XmnI presented a single band at 2600 bp, which corresponds to the expected size of pUC18-His.

Mutants of mNeonGreen were generated through EP-PCR.

To identify mutations in mNeonGreen EP-PCR products, two mutants were sequenced. In the M4 mutant, one single mutation was identified: I67T. In the M3 mutant, three mutations were identified: L19M, A192V & M231V. The M4 mutant's I67T mutation was found to be located near the mNeonGreen chromophore and to disrupt folding in this region (Fig. 4). On the other hand, the M3 mutant's L19M mutation was located in the β-barrel and did not affect

folding, nor did the A192V mutation which was located in a loop (Fig. 4). The M3 mutant's M231V mutation was not located and its effect on protein folding was not assessed, as it was not present in the model that was used for the analysis.

M4 mNeonGreen mutant has a lower level of expression compared to wildtype mNeonGreen protein expression levels.

To determine how protein expression of M3 and M4 mNeonGreen mutants compares to wildtype mNeonGreen, Western blot detection of the protein was performed. Then, signal density of the mNeonGreen bands was analysed to assess protein expression. Signal density of the M3 and wildtype mNeonGreen was similar (Fig. 5B). On the other hand, the M4 band signal expression was less than half that of wildtype mNeonGreen (Fig. 5B). No bands were observed in the lanes with no mNeonGreen protein (Fig 5A).

M4 mNeonGreen mutant has a significantly different fluorescence intensity, excitation maximum, emission maximum, pKa and bleaching half-time compared to wildtype mNeonGreen.

Spectrofluorometric data obtained for purified wildtype, M3 and M4 mNeonGreen proteins shows that wildtype and M3 mNeonGreen proteins have similar fluorescent intensities, while M4 has reduced fluorescent intensity ($p < 0.05$) (Fig. 6A,F,G). Additionally, wildtype and M3 mNeonGreen have similar excitation and emission maximum wavelengths, while M4 has smaller excitation (Fig. 6B,F) and emission wavelengths (Fig. 6C,G) ($p < 0.05$). Although they have different maxima, the overall shapes of the excitation and emission spectral curves remained similar for all mNeonGreen variants (Fig. 6F,G).
Moreover, pKa and bleaching half-time of the mNeonGreen protein variants were measured to assess their stability characteristics. The pKa of the wildtype and M3 mNeonGreen mutants were not significantly different. However, the pKa of the M4 mNeonGreen mutant was significantly higher than that of the wildtype ($p < 0.05$) (Fig. 6D). On the other hand, the bleaching half-time of wildtype and M3 mNeonGreen mutants were similar, but the bleaching half-time of the M4 mutant was significantly longer than that of the wild type by approximately 1.4 seconds ($p < 0.05$) (Fig. 6E).

(786 words)

Figures

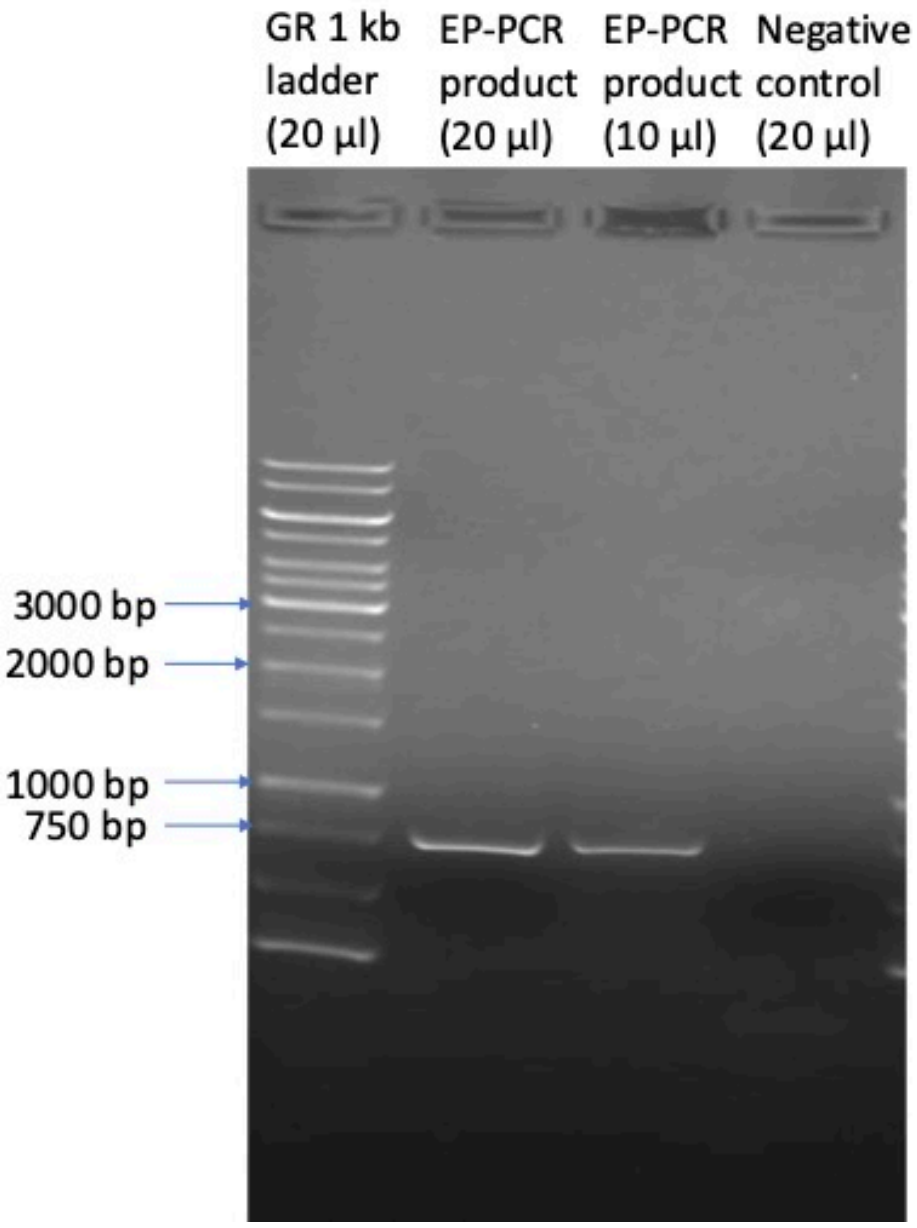

Figure 1. mNeonGreen was Amplified by Error Prone PCR. Agarose gel electrophoresis of EP-PCR product. Lane 1: GeneRuler 1 kb DNA ladder. Lane 2: 20 µl of EP-PCR product. Lane 3: 10 µl of EP-PCR product. Lane 4: 20 µl of no template negative control. Bands at approximately 720 bp present in lanes 2 and 3 correspond to the size of the mNeonGreen gene.

A

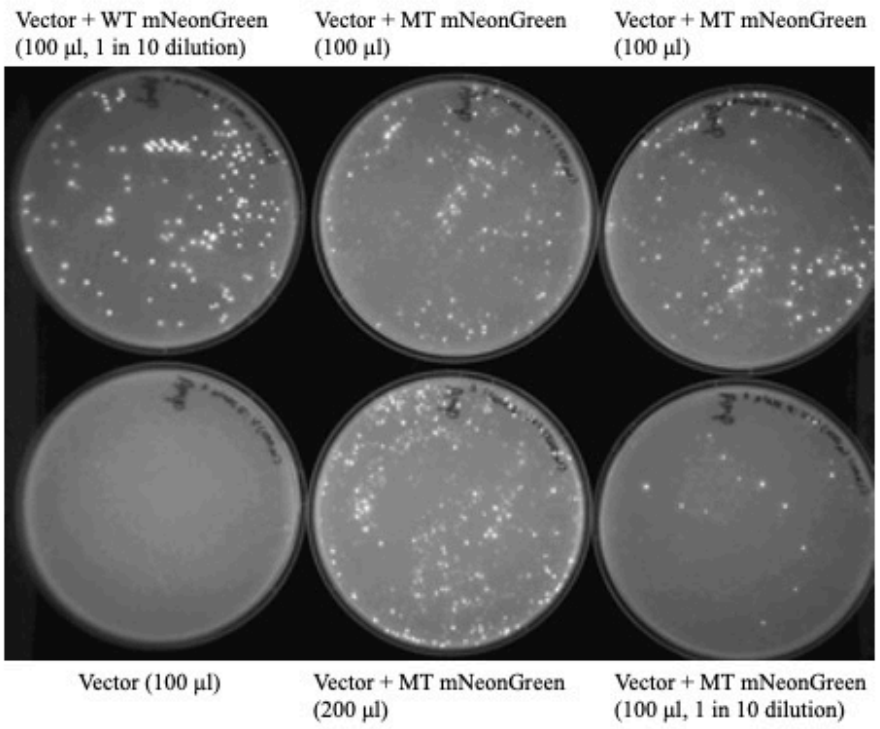

B

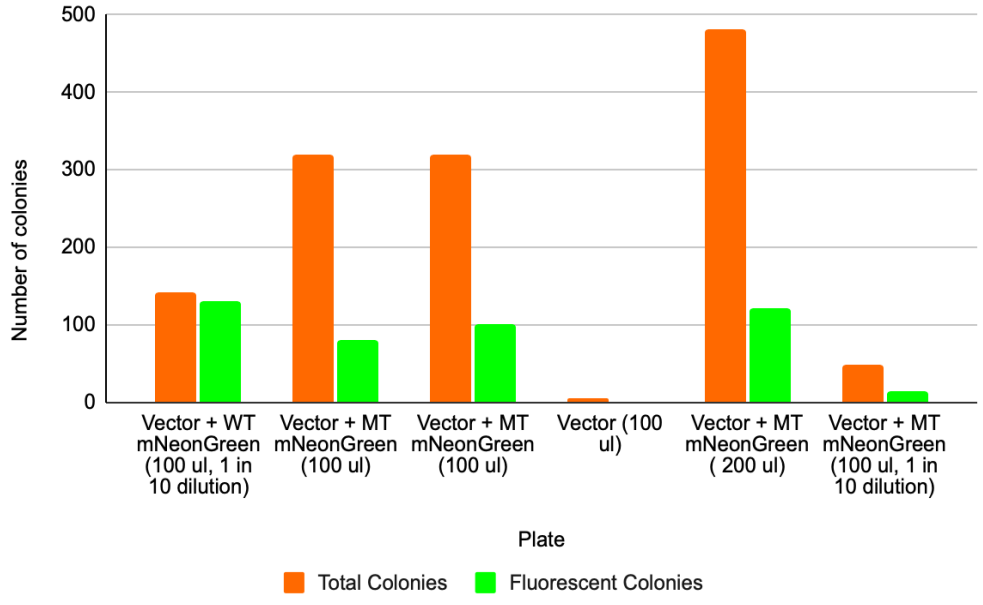

Figure 2. mNeonGreen EP-PCR products were cloned into *E. coli.* (A) Bacterial colonies transformed with pUC18-His-mNeonGreen vectors selected on LB agar plates containing ampicillin imaged using ChemiDoc. (B) Total colony and fluorescent colony number in plates.

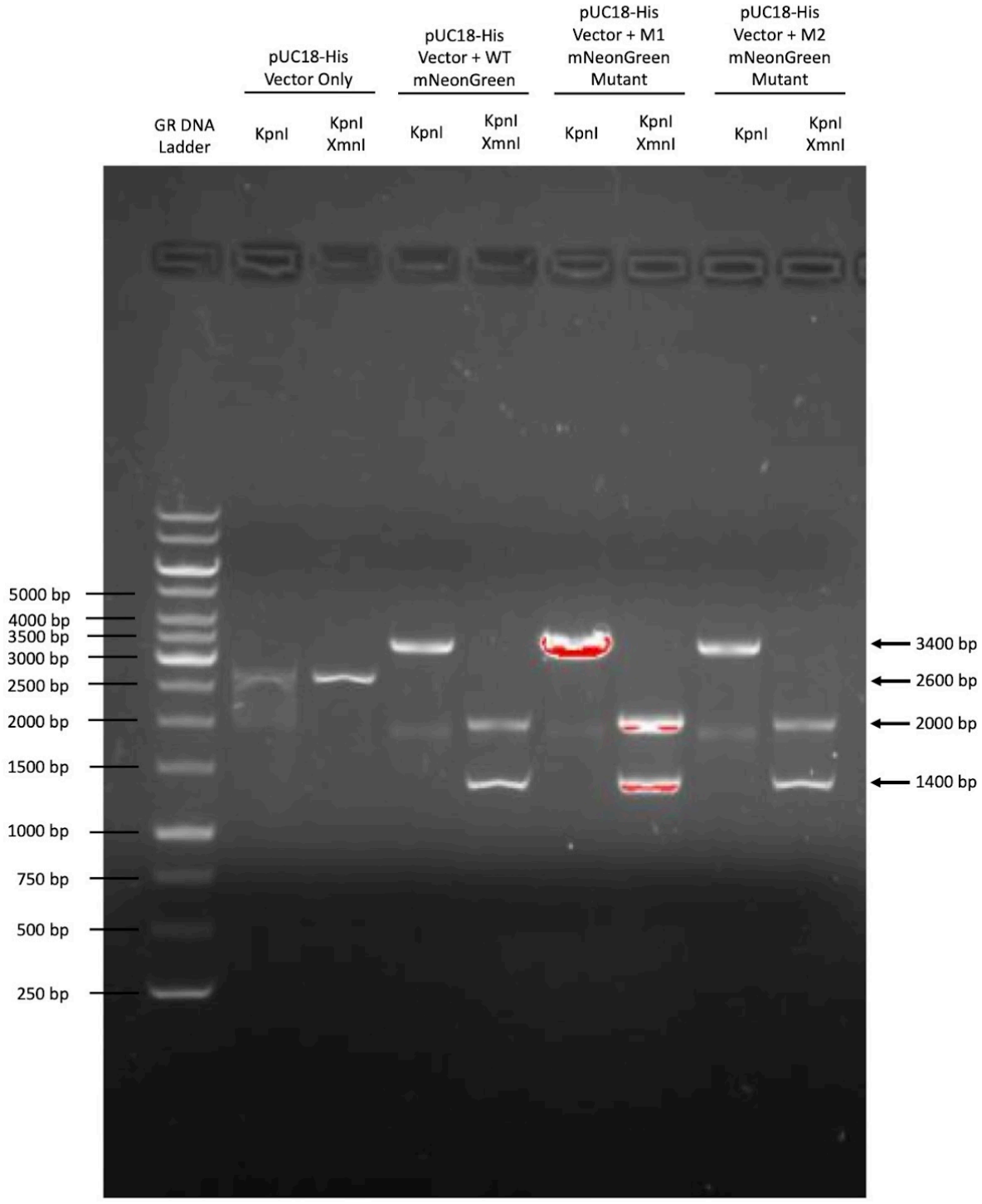

Figure 3. mNeonGreen EP-PCR products were ligated into pUC18-His plasmid vector. Agarose gel electrophoresis of restriction enzyme digests of the plasmid vectors. Lane 1: GeneRuler DNA ladder. Lane 2: pUC18-His vector digested with KpnI enzyme. Lane 3: pUC18-His vector digested with KpnI and XmnI enzymes. Lanes 4, 6, 8: pUC18-His-mNeonGreen variant vectors digested with KpnI. Lanes 5, 7, 9: pUC18-His-mNeonGreen variant vectors digested with KpnI and XmnI. Bands at 2600 bp correspond to the size of empty pUC18-His vectors. Bands at 3400 bp correspond to the size of pUC18-His vector with mNeonGreen variants.

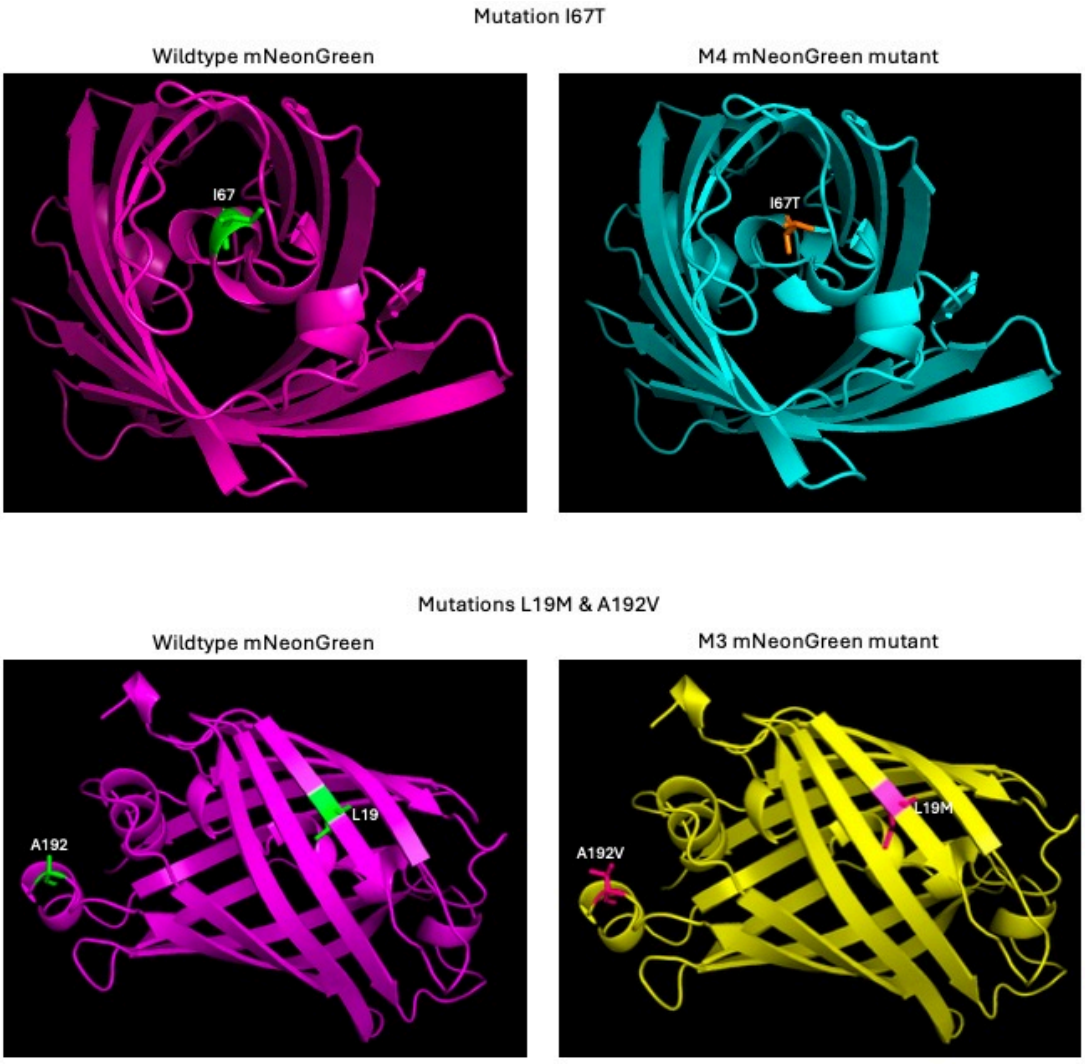

Figure 4. EP-PCR generated mutants of mNeonGreen. Modelling of wildtype and mutant mNeonGreen with PyMol. The M4 mutation is I67T, located near the chromophore. It changes the folding in the region in this model. The M3 mutations are L19M and A192V, located in the β-barrel and in a loop respectively and they do not change the folding according to the model.

A. B.

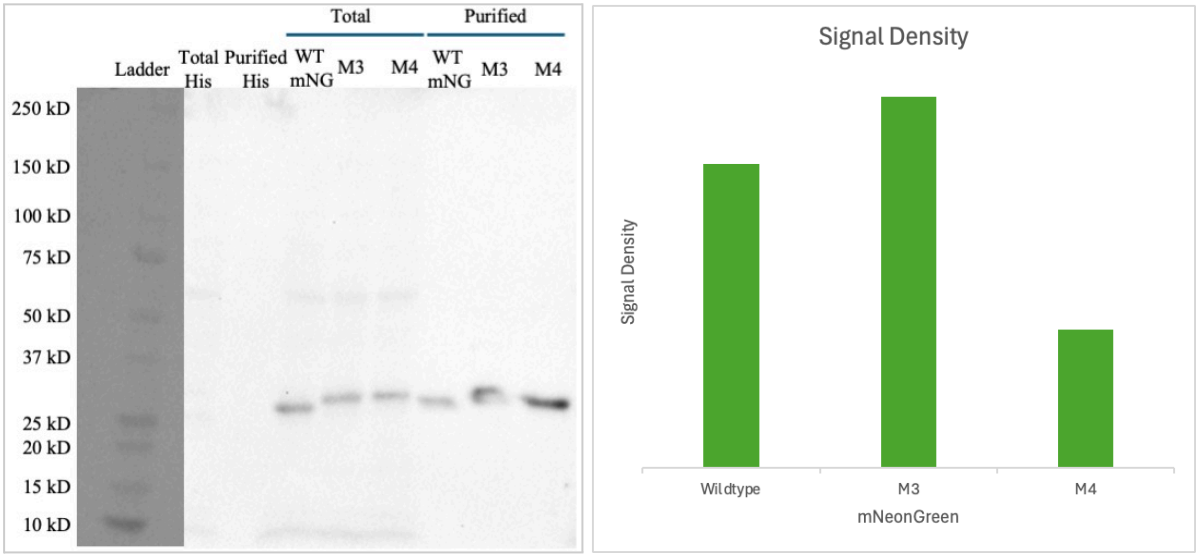

Figure 5. Wildtype and M3 mNeonGreen have similar expression levels, while M4 has lower protein expression levels. (A) Western blot detection of wildtype, M3 and M4 mutant mNeonGreen in total and purified protein lysates, as well as 6xHis tag only protein lysates. (B) Signal intensity of Western blot detection bands of wildtype, M3 and M4 mutant mNeonGreen.

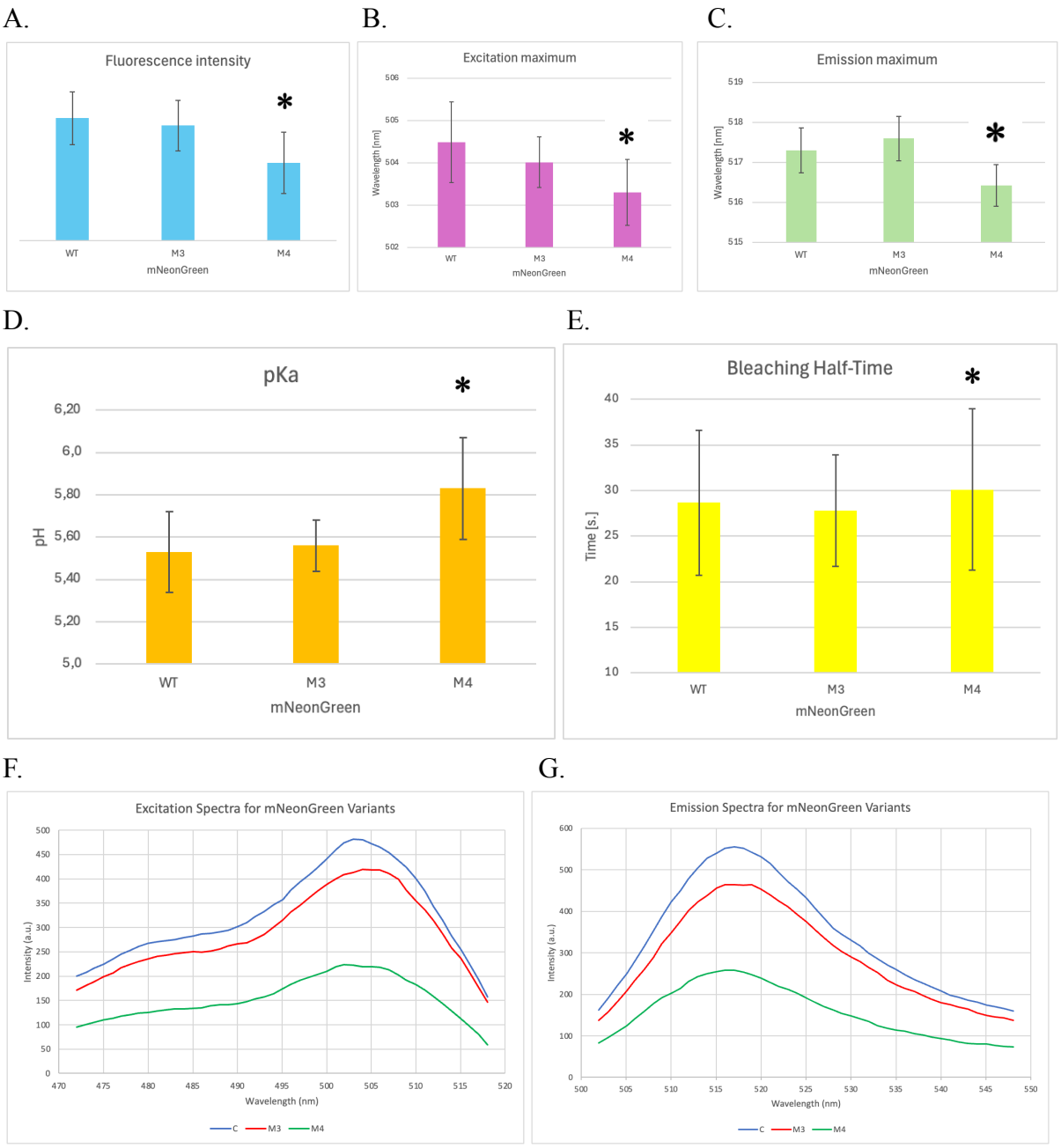

Figure 6. Wildtype and M3 mNeonGreen have similar fluorescence intensity, spectral properties and stability, while M4 has lower fluorescence intensity, blueshifted excitation and emission spectra, higher pKa and longer bleaching half-time. (A) Fluorescence intensities of purified mNeonGreen variants. (B) Excitation maxima of purified mNeonGreen variants. (C) Emission maxima of purified mNeonGreen variants. (D) pKa of purified mNeonGreen variants. (E) Bleaching half-time of mNeonGreen variants. (F) Excitation spectra of mNeonGreen variants. (G) Emission spectra of mNeonGreen variants.

Discussion

This study investigated whether random mutagenesis of mNeonGreen through EP-PCR could generate variants with altered fluorescent properties and stability. Overall, the results show that the mutagenesis in our M3 was relatively neutral, while the variant M4 showed significant detrimental changes in the outcome. These findings confirm that random substitutions can impact fluorescent properties, however, beneficial improvements were not observed under the tested conditions.

Initial mutagenesis and cloning steps produced a diverse library and was confirmed to successfully express fluorescent proteins in *E. coli*. The presence of colonies with varying fluorescence illustrated how mutations affected protein behavior under bacterial conditions. This outcome is expected from prior work, showing that random and targeted mutations in the β-barrel scaffold will typically affect folding, chromophore maturation, and fluorescence efficiency.[5,6,9]

Sanger sequencing revealed that the M3 carried three amino-acid substitutions (L19M, A192V, M231V), while the M4 had a single substitution (I67T). I67T lies close to the chromophore pocket, whereas the mutations in M3 reside more in the peripheral regions of the β-barrel or loops. Past mutational studies related to fluorescent proteins indicate that substitutions within or near the chromophore frequently alter excitation/emission spectra, quantum yield, pH-sensitivity, or photostability, whereas more distant substitutions have milder effects.[6,9] Thus, the different mutation contexts provide the explanation for why the M4 was significantly different from the wild-type mNeonGreen, while M3 was not.

Purified-protein assays confirmed these structural predictions. For M3, all metrics were essentially identical to wild-type, indicating that the substitutions did not affect the chromophore chemistry or barrel integrity. For M4, fluorescence intensity dropped, excitation and emission spectra were blue-shifted, pKa increased, and the bleaching half-time lengthened. The spectral shift and change in pKa suggest that I67T may have changed the chromophore's local electrostatic hydrogen-bond network which is consistent with many studies proving that even a single point mutation in the chromophore can dramatically alter photophysical behavior.[6,9] In particular, M4 showed a significant reduction in fluorescence intensity and significant shifts in excitation and emission maxima compared to the wild-type ($p < 0.05$) (Fig. 6A-C).

The Western blot data showed that M4 expresses at significantly lower levels than wild-type or M3, indicating that part of its reduced fluorescence is likely due to lower protein yield, not entirely altered chromophore behavior. Prior studies of GFP variants have also reported that misfolding and inefficient maturation can underlie decreased fluorescence and stability.[2,5,6] Thus, the phenotype of M4 likely reflects the combination of impaired folding/stability, altered chromophore environment, and reduced expression.

Although this first round of mutagenesis did not yield a significantly brighter variant, the results are still valuable. Complex traits such as fluorescence brightness, stability, and maturation often need multiple iterative rounds to accumulate beneficial substitutions while eliminating deleterious ones.[4,7,8] Additionally, engineering efforts of other fluorescent proteins have typically processed through multiple cycles of mutagenesis and screening before achieving improved performance.[7,8] The observation that M3 remained functionally equivalent to the wild-type shows that its substitutions were tolerated, which could act epistatically or additively with future mutations. In contrast, M4's detrimental phenotype identifies a residue that likely should be avoided in future rounds.

Future experiments should include additional rounds of mutagenesis targeting chromophore-proximal or structurally important residues. This should include high-throughput fluorescence-based screening using flow cytometry or plate readers, and more comprehensive in vitro characterization, including yield and photostability. It can be noted that achieving modest improvements could substantially benefit applications such as live-cell imaging, biosensing, and FRET, where small fluorescence or stability gains greatly improve signal sensitivity.[1,2,9] More broadly, shifts in pKa and photobleaching behavior can directly affect imaging performance by changing signal stability across pH ranges and under continuous illumination. (Fig. 6D-E)

In conclusion, this work demonstrates how random mutagenesis can produce mNeonGreen variants with altered fluorescence properties and stability, confirming that the sequence space around this protein is modifiable. While none of the variants surpasses the wild-type in brightness or stability in this first round, this data provides a foundation for iterative evolution. All together, these findings support the hypothesis that random substitutions can modulate fluorescent protein behavior and outline a clear path toward improving mNeonGreen for advanced imaging applications.

(700 words)

References

[1] Cranfill, P.J., Sell, B.R., Baird, M.A., Allen, J.R., Lavagnino, Z., de Gruiter, H.M., Kremers, G.-J., Davidson, M.W., Ustione, A., and Piston, D.W. (2016). Quantitative assessment of fluorescent proteins. Nat. Methods 13, 557 –562. 10.1038/nmeth.3891.

[2] Shaner, N.C., Lambert, G.G., Chammas, A., Ni, Y., Cranfill, P.J., Baird, M.A., Sell, B.R., Allen, J.R., Day, R.N., Israelsson, M., Davidson, M.W., and Wang, J. (2013). A bright monomeric green fluorescent protein derived from *Branchiostoma lanceolatum*. Nat. Methods 10, 407–409. 10.1038/nmeth.2413.

[3] Shaner, N.C., Lin, M.Z., McKeown, M.R., Steinbach, P.A., Hazelwood, K.L., Davidson, M.W., and Tsien, R.Y. (2008). Improving the photostability of bright monomeric orange and red fluorescent proteins. *Nat. Methods* **5**, 545–551. 10.1038/nmeth.1209.

[4] Cadwell, R.C., and Joyce, G.F. (1992). Randomization of genes by PCR mutagenesis. *PCR Methods Appl.* **2**, 28–33. 10.1101/gr.2.1.28.

[5] Pédelacq, J.-D., Cabantous, S., Tran, T., Terwilliger, T.C., and Waldo, G.S. (2006). Engineering and characterization of a superfolder green fluorescent protein. *Nat. Biotechnol.* 24, 79–88. https://doi.org/10.1038/nbt1172.

[6] Remington, S.J. (2006). Fluorescent proteins: maturation, photochemistry and photophysics. *Curr. Opin. Struct. Biol.* 16, 714–721. https://doi.org/10.1016/j.sbi.2006.10.001.

[7] Kiss, C., Temirov, J., Chasteen, L., Waldo, G.S., and Bradbury, A.R.M. (2009). Directed evolution of an extremely stable fluorescent protein. *Protein Eng. Des. Sel.* 22, 313–323. https://doi.org/10.1093/protein/gzp006.

[8] Sachsenhauser, V., and Bardwell, J.C.A. (2018). Directed evolution to improve protein folding in vivo. *Curr. Opin. Struct. Biol.* 48, 117–123. https://doi.org/10.1016/j.sbi.2017.12.003.

[9] Rodríguez, E.A., Campbell, R.E., Lin, J.Y., et al. (2017). The Growing and Glowing Toolbox of Fluorescent and Photoactive Proteins. *Trends Biochem. Sci.* 42, 111–129. https://doi.org/10.1016/j.tibs.2016.09.010.